

# HAT-P-3b: A heavy-element rich planet transiting a K dwarf star

G. Torres<sup>1</sup>, G. Á. Bakos<sup>1,2</sup>, G. Kovács<sup>3</sup>, D. W. Latham<sup>1</sup>, J. M. Fernández<sup>1</sup>, R. W. Noyes<sup>1</sup>,  
G. A. Esquerdo<sup>1</sup>, A. Sozzetti<sup>1,4</sup>, D. A. Fischer<sup>5</sup>, R. P. Butler<sup>6</sup>, G. W. Marcy<sup>7</sup>, R. P.  
Stefanik<sup>1</sup>, D. D. Sasselov<sup>1</sup>, J. Lázár<sup>8</sup>, I. Papp<sup>8</sup>, P. Sári<sup>8</sup>

## ABSTRACT

We report the discovery of a Jupiter-size planet transiting a relatively bright ( $V = 11.56$ ) and metal-rich early K dwarf star with a period of  $\sim 2.9$  days. On the basis of follow-up photometry and spectroscopy we determine the mass and radius of the planet, HAT-P-3b, to be  $M_p = 0.599 \pm 0.026 M_{\text{Jup}}$  and  $R_p = 0.890 \pm 0.046 R_{\text{Jup}}$ . The relatively small size of the object for its mass implies the presence of about  $75 M_{\oplus}$  worth of heavy elements ( $\sim \frac{1}{3}$  of the total mass) based on current theories of irradiated extrasolar giant planets, similar to the mass of the core inferred for the transiting planet HD 149026b. The bulk density of HAT-P-3b is found to be  $\rho_p = 1.06 \pm 0.17 \text{ g cm}^{-3}$ , and the planet orbits the star at a distance of 0.03894 AU. Ephemerides for the transit centers are  $T_c = 2,454,218.7594 \pm 0.0029 + N \times (2.899703 \pm 0.000054)$  (HJD).

*Subject headings:* binaries: spectroscopic — planetary systems — stars: fundamental parameters — stars: individual (HAT-P-3) — techniques: spectroscopic

## 1. Introduction

Ground-based surveys for extrasolar transiting planets have produced 18 discoveries to date. This sample is still small enough that individual discoveries often advance our

---

<sup>1</sup>Harvard-Smithsonian Center for Astrophysics, Cambridge, MA, gtorres@cfa.harvard.edu

<sup>2</sup>Hubble Fellow

<sup>3</sup>Konkoly Observatory, Budapest, P.O. Box 67, H-1125, Hungary

<sup>4</sup>INAF - Osservatorio Astronomico di Torino, 10025 Pino Torinese, Italy

<sup>5</sup>Department of Physics and Astronomy, San Francisco State University, San Francisco, CA

<sup>6</sup>Department of Terrestrial Magnetism, Carnegie Institute of Washington, DC

<sup>7</sup>Department of Astronomy, University of California, Berkeley, CA

<sup>8</sup>Hungarian Astronomical Association, Budapest, Hungary

understanding of these objects significantly by pushing the limits of parameter space, either in planet mass, radius, or some other property. Here we announce a new transiting planet, the third to come out of the HATNet survey, around a star previously known as GSC 03466-00819. It is the smallest yet discovered photometrically, and appears to have a heavy-element content representing a substantial fraction of its mass.

## 2. Photometric detection

GSC 03466-00819 is located in our internally labeled field “G145” centered at  $\alpha = 13^{\text{h}}48^{\text{m}}$ ,  $\delta = +45^{\circ}00'$ , which was observed using the 11-cm aperture HAT-5 instrument of the HAT network (HATNet; Bakos et al. 2002, 2004), located at the F. L. Whipple Observatory (FLWO) on Mt. Hopkins (Arizona). The field was observed in single-station mode, i.e., without networked operations between Arizona and HATNet’s other station in Hawaii. Observations over an extended interval of six months (from 2006 January 28 through 2006 July 22) yielded some 3200 photometric measurements per star for approximately 10,000 stars in the field down to  $I \sim 14$ . Following standard frame calibration procedures astrometry was performed as described in Pál & Bakos (2006), and aperture photometry results were subjected to the de-trending algorithms we refer to as External Parameter Decorrelation (EPD, described briefly in Bakos et al. 2007), and Trend Filtering Algorithm (TFA; Kovács et al. 2005). We searched the light curves for box-shaped transit signals using the BLS algorithm of Kovács et al. (2002). A prominent 2.9-day signal was detected in the  $I \approx 10.52$  magnitude star GSC 03466-00819 (also known as 2MASS 13442258+4801432;  $\alpha = 13^{\text{h}}44^{\text{m}}22^{\text{s}}.58$ ,  $\delta = +48^{\circ}01'43''.2$ ; J2000) with a transit depth of 0.014 mag and a dip-significance parameter (DSP) of  $\sim 11$  (Kovács & Bakos 2005). This discovery light curve is shown in Figure 1a. The standard deviation of the measurements after the EPD procedure was 0.009 mag. Altogether 5 partial and 2 full transits were observed. As is shown in the following sections the transiting companion is a Jovian planet. Hereafter we refer to the star as HAT-P-3, and to the planetary companion as HAT-P-3b.

The near infrared color of the star ( $J-K_s = 0.49$ ) corresponds to an early K dwarf, and the annual proper motion listed in the Tycho-2 catalog ( $\mu_\alpha \cos \delta = -23.3 \pm 2.9$  mas yr $^{-1}$ ,  $\mu_\delta = -24.0 \pm 2.6$  mas yr $^{-1}$ ; Høg et al. 2000) is consistent with this. The photometric ephemeris was determined by combining all recorded HATNet transit events with a full transit observed more recently at higher precision with a larger telescope, as described below. The period we obtain is  $P = 2.899703 \pm 0.000054$  days, and the reference epoch of transit center is  $T_c = 2,454,218.7594 \pm 0.0029$  (HJD). We use this ephemeris for the remainder of the paper.

We note that HAT-P-3 has a faint ( $I \approx 15$ ) and red ( $J - K_s = 0.86$ ) companion at an angular separation of  $\sim 10''$  (2MASS 13442345+4801387), which is entirely within the aperture used for the HATNet photometry. If this happened to be an eclipsing binary, we estimate, based on the relative fluxes, that 1.6-mag deep eclipses of this star could mimic the observed shallow transits seen in the merged light curve. However, our follow-up photometry described in §3 with much better spatial resolution shows that the shallow dips in brightness are indeed present in the light curve of HAT-P-3, whereas the faint companion is constant at the 0.05 mag level.

### 3. Follow-up observations

HAT-P-3 was observed spectroscopically with the FLWO 1.5-m Tillinghast reflector in order to rule out the possibility that the observed drop in brightness is caused by a stellar companion in an eclipsing binary. Three spectra were obtained with the CfA Digital Speedometer (Latham 1992) over an interval of 25 days. These observations cover 45 Å in a single echelle order centered at 5187 Å, and have a resolving power of  $\lambda/\Delta\lambda \approx 35,000$ . Radial velocities were obtained by cross-correlation and have a typical precision of  $0.4 \text{ km s}^{-1}$ . They showed no variation within the uncertainties, ruling out a companion of stellar mass. The mean velocity is  $-23.8 \pm 0.1 \text{ km s}^{-1}$ .

Higher resolution spectroscopy was conducted with the HIRES instrument (Vogt et al. 1994) on the Keck I telescope. With a spectrometer slit of  $0''.86$  the resolving power is  $\lambda/\Delta\lambda \approx 55,000$ , and the wavelength coverage is  $\sim 3800\text{--}8000 \text{ Å}$ . An iodine gas absorption cell was used to superimpose a dense forest of  $I_2$  lines on the stellar spectrum and establish a highly accurate wavelength fiducial (see Marcy & Butler 1992). A total of nine 12-minute exposures were obtained between 2007 March and June with the iodine cell, along with one without  $I_2$  for use as a template. Relative radial velocities in the Solar System barycentric frame were derived as described by Butler et al. (1996), including full modeling of the spatial and temporal variations of the instrumental profile. The results, listed in Table 1, have internal errors  $\lesssim 3 \text{ m s}^{-1}$ .

The iodine-free template spectrum from Keck was used to infer the atmospheric parameters of the star. A spectral synthesis modeling was carried out using the SME software (Valenti & Piskunov 1996), with wavelength ranges and atomic line data as described by Valenti & Fischer (2005). The effective temperature ( $T_{\text{eff}}$ ), surface gravity ( $\log g_*$ ), iron abundance ( $[\text{Fe}/\text{H}]$ ), and projected rotational velocity ( $v \sin i$ ) we obtain are listed in Table 2, where the uncertainties represent internal errors. The temperature and surface gravity correspond to an early K dwarf.

Photometric follow-up of HAT-P-3 was carried out in the Sloan  $i$  band with KeplerCam (see Holman et al. 2007) on the 1.2-m telescope at FLWO. After several attempts thwarted by weather we obtained a reasonably complete and high-precision light curve of HAT-P-3 on UT 2007 April 27. An astrometric solution between the individual frames and the 2MASS catalog was carried out using first order polynomials based on  $\sim 100$  stars per frame. Aperture photometry was performed using a series of apertures on fixed positions around the 2MASS-based  $[X, Y]$  pixel coordinates. We selected a frame taken near the meridian and used  $\sim 70$  stars and their magnitudes as measured on this reference frame to transform all other frames to a common instrumental magnitude system (weighting by the estimated photometric errors of each star). The aperture yielding the lowest scatter outside of transit was used in the subsequent analysis. The light curve of HAT-P-3 (Figure 1b) was then de-correlated against trends using the out-of-transit sections and a dependence on hour angle and zenith distance. The photometry is somewhat affected by occasional thin cirrus during the night, and has a typical precision of  $\sim 2.5$  mmag per individual measurement at 20-second cadence.

#### 4. Analysis

Modeling of the  $i$ -band light curve was carried out using the formalism of Mandel & Agol (2002). Quadratic limb-darkening coefficients ( $u_1 = 0.3832$  and  $u_2 = 0.2683$ ) were taken from the tables of Claret (2004) by interpolation to the stellar properties given in Table 2. The period was held fixed, and the orbit was assumed to be circular, since the eccentricity is not sufficiently well constrained by the presently available velocity measurements. The four adjusted parameters are the planet-to-star ratio of the radii ( $R_p/R_\star$ ), the normalized separation ( $a/R_\star$ ) where  $a$  is the semimajor axis of the relative orbit, the impact parameter ( $b \equiv a \cos i/R_\star$ ), and the time of the center of the transit ( $T_c$ ). A grid search was performed at a fixed  $T_c$  to locate the  $\chi^2$  minimum in the parameter space of the other three variables, and these were subsequently held fixed to optimize  $T_c$ . The process was iterated until convergence. Uncertainties were estimated by alternately fixing each parameter at a range of values near the minimum and allowing the others to float, until the best-fit solution produced an increase in the  $\chi^2$  corresponding to a  $1\sigma$  change. The results are shown in Table 3.

The relative radial velocities of HAT-P-3 were fitted with a Keplerian model constrained to have zero eccentricity. The ephemeris was held fixed at the value for  $P$  determined in §2 and  $T_c$  from the light curve analysis. The solution fits the data well (see Figure 2a), but has an rms scatter of  $4.7 \text{ m s}^{-1}$  (accounting for the number of degrees of freedom) that is larger than the typical internal errors ( $1.3\text{--}2.9 \text{ m s}^{-1}$ ). No obvious long-term trends are

seen in the residuals. Inspection of the spectra reveals that the Ca II H and K lines display modest emission cores, indicative of a small degree of chromospheric activity. This is known to cause excess scatter in the velocities (e.g., Saar & Donahue 1997), and is often referred to as “jitter”. While we cannot rule out other systematics that may be causing our internal errors to be underestimated, we attribute most of the excess scatter to activity. For our final fit we have added  $4.2 \text{ ms}^{-1}$  in quadrature to our formal errors, which yields a reduced  $\chi^2$  near unity. The parameters of the fit are not significantly changed, and are listed in Table 3. The minimum companion mass is  $M_p \sin i = 0.625 \pm 0.015 \times [(M_\star + M_p)/M_\odot]^{2/3} M_{\text{JUP}}$ , where  $M_\star$  represents the mass of the star.

We investigated the possibility that the radial velocities we measured are the result of distortions in the line profiles due to contamination from an unresolved eclipsing binary (Santos et al. 2002; Torres et al. 2005), instead of being due to true Doppler motion in response to a planetary companion. We cross-correlated each Keck spectrum against a synthetic template matching the properties of the star, and averaged the correlation functions over all orders blueward of the region affected by the iodine lines. From this representation of the average spectral line profile we computed the mean bisectors, and as a measure of the line asymmetry we calculated the “bisector spans” as the velocity difference between points selected near the top and bottom of the mean bisectors (Torres et al. 2005). If the velocities were the result of a blend with an eclipsing binary, we would expect the line bisectors to vary in phase with the photometric period with an amplitude similar to that of the velocities (Queloz et al. 2001; Mandushev et al. 2005). Instead, we detect no variation in excess of the measurement uncertainties (see Figure 2, bottom panel). We conclude that the velocity variations are real and that the star is orbited by a Jovian planet.

## 5. Star and planet parameters

The mass and radius of the planetary companion scale with those of the parent star. We have estimated the stellar properties by comparison with stellar evolution models from the Yonsei-Yale ( $Y^2$ ) series by Yi et al. (2001). However, because a direct estimate of the distance is unavailable (HAT-P-3 was not observed during the *Hipparcos* mission), we have used as a proxy for luminosity ( $L_\star$ ) the quantity  $a/R_\star$  from the light curve fit, which is closely related to the stellar density (see Sozzetti et al. 2007). As described by those authors,  $a/R_\star$  is typically a better constraint on  $L_\star$  than the spectroscopic value of  $\log g_\star$ , which has a relatively subtle effect on the line profiles and whose determination is therefore more susceptible to systematic errors. Following Sozzetti et al. (2007) we have determined the range of stellar masses and radii that are consistent with the measured values of  $T_{\text{eff}}$ ,  $[\text{Fe}/\text{H}]$ , and  $a/R_\star$  within their

uncertainties. Based on previous experience, for this application we have adopted more conservative errors for the spectroscopic quantities of 80 K for  $T_{\text{eff}}$  and 0.08 dex for [Fe/H]. We obtain  $M_{\star} = 0.936^{+0.036}_{-0.062} M_{\odot}$  and  $R_{\star} = 0.824^{+0.043}_{-0.035} R_{\odot}$ . The predicted surface gravity,  $\log g_{\star} = 4.577^{+0.019}_{-0.045}$ , agrees well with the spectroscopic estimate (see Table 2). The nominal age we infer for HAT-P-3 is only 0.4 Gyr, although the uncertainty is very large due to the unevolved nature of this K dwarf. While this nominal age would make HAT-P-3 the youngest known transiting extrasolar planet host star, we note that there is no sign of the Li I  $\lambda 6708$  line in the spectra of HAT-P-3 down to a factor of  $\sim 4$  lower than the Li level in stars of similar spectral type in the Hyades cluster, which have an age of  $\sim 0.7$  Gyr. This would suggest an age for HAT-P-3 greater than 0.7 Gyr. Further evidence for an older age is provided by the measured chromospheric activity index of the star based on the Ca II H and K lines in the Keck spectra:  $\log R'_{\text{HK}}$  is  $-4.59 \pm 0.06$ , indicating an age of  $\sim 1.3$  Gyr based on the calibration by Noyes et al. (1984).

Combined with the results from the light curve and radial velocity modeling, the above stellar parameters yield a planet mass of  $M_p = 0.599 \pm 0.026 M_{\text{Jup}}$  and a radius of  $R_p = 0.890 \pm 0.046 R_{\text{Jup}}$ . The surface gravity of the planet, which is independent of the stellar parameters (see, e.g., Southworth et al. 2007), is  $\log g_p = 3.310 \pm 0.066$  (cgs), and is consistent with the  $P/\log g_p$  relation shown by those authors. These and other planet properties are listed in Table 3.

The absolute visual magnitude we estimate for the star using the stellar evolution models ( $M_V = 5.86 \pm 0.20$ ) combined with the apparent visual magnitude ( $V = 11.561 \pm 0.067$ ; Droege et al. 2006) yields a distance of  $140 \pm 13$  pc, ignoring extinction. With this distance estimate we investigated the possibility that the faint  $10''$  companion to HAT-P-3 mentioned in §2 is physically associated. We find that it is not: its  $K_s$ -band brightness as measured by 2MASS is approximately 2 magnitudes fainter than predicted for a star with its  $J-K_s$  color, using the best-fit isochrone to HAT-P-3. It is therefore a background star.

## 6. Discussion and concluding remarks

The properties of HAT-P-3b place it among the smaller transiting planets discovered so far, and are remarkably similar to those of the recently announced XO-2b (Burke et al. 2007), not only in mass and radius (reported as  $0.57 M_{\text{Jup}}$  and  $0.97 R_{\text{Jup}}$ , respectively), but also in some of the characteristics of the parent star such as  $T_{\text{eff}}$  and  $M_{\star}$ . In the case of HAT-P-3b, with a mass of  $M_p = 0.599 M_{\text{Jup}}$ , the radius measured here appears too small for a pure hydrogen-helium planet according to current theory. The models for irradiated giant planets by Fortney et al. (2007) indicate the radius could be explained by the presence of a heavy-

element core of some  $75 M_{\oplus}$  ( $\sim \frac{1}{3}$  of the total  $M_p$ ) for the nominal mass, orbital semimajor axis, and age we infer, although uncertainties in these properties and in the planetary radius allow the range to be from about 50 to  $100 M_{\oplus}$ . HAT-P-3b thus joins HD 149026b (Sato et al. 2005) as a hot Jupiter for which theory predicts a substantial fraction of heavy elements. Using the same models and the published properties of XO-2b, we find that XO-2b is also expected to have a  $40 M_{\oplus}$  core representing about  $\frac{1}{4}$  of its total mass. These three heavy-element rich planets, along with others suggested by Burrows et al. (2007), provide important support for the core-accretion scenario of planet formation. HAT-P-3b appears consistent with the correlation proposed by Guillot et al. (2006) between the host star metallicity and the amount of heavy elements in the planet interior, although there seems to be at least one exception to this relation (WASP-1b; Stempels et al. 2007). Compared to HD 149026b, HAT-P-3b has a similar mass of heavy elements but considerably more hydrogen and helium, a feature that will need to be explained by planet formation models.

As of this writing HAT-P-3b is the smallest extrasolar transiting planet discovered photometrically. While HD 149026b and GJ 436b (Gillon et al. 2007) do have smaller radii, they were both originally discovered in Doppler surveys before transits were noticed.

Gaudi (2005) has argued that selection effects in signal-to-noise-limited transit surveys tend to bias the size distribution of close-in giant extrasolar planets toward larger radii, since those objects have deeper transits and are therefore easier to detect. The fact that the recent discoveries of HAT-P-3b and XO-2b are on the small side of the radius distribution would seem to contradict the argument. However, the transit depth in both of these cases is not particularly small ( $\sim 1.4\%$ ), a result of the fact that the parent stars are K dwarfs rather than earlier type stars. Thus, there may still be a bias, although relatively small. We note also that the properties of HAT-P-3b are entirely consistent with the Monte Carlo simulations of the population of transiting planets by Fressin et al. (2007) (see, e.g., their Fig. 17), as are other recently announced transiting planets. This supports the idea that these objects are quite representative of the general population of giant planets, and are not significantly different from the Doppler planets.

We are grateful to the referee, T. Guillot, for helpful comments on the original manuscript. Operation of the HATNet project is funded in part by NASA grant NNG04GN74G. We acknowledge partial support also from the Kepler Mission under NASA Cooperative Agreement NCC2-1390 (D.W.L., PI). G.T. acknowledges partial support from NASA under grant NNG04LG89G, and work by G.Á.B. was supported by NASA through Hubble Fellowship Grant HST-HF-01170.01-A. G.Á.B. also wishes to acknowledge the use of the photometry software that is under development by A. Pál. G.K. thanks the Hungarian Scientific Research Foundation (OTKA) for support through grant K-60750. This research has made

use of Keck telescope time granted through NASA, of the VizieR service (Ochsenbein et al. 2000) operated at CDS, Strasbourg, France, of NASA’s Astrophysics Data System Abstract Service, and of the 2MASS Catalog.

## REFERENCES

- Bakos, G. Á., Lázár, J., Papp, I., Sári, P., & Green, E. M. 2002, *PASP*, 114, 974
- Bakos, G. Á., Noyes, R. W., Kovács, G., Stanek, K. Z., Sasselov, D. D., & Domsa, I. 2004, *PASP*, 116, 266
- Bakos, G. Á., et al. 2007, *ApJ*, submitted (arXiv:0705.0126)
- Burrows, A., Hubeny, I., Budaj, J., & Hubbard, W. B. 2007, *ApJ*, 661, 502
- Butler, R. P., Marcy, G. W., Williams, E. et al. 1996, *PASP*, 108, 500
- Burke, C. J. et al. 2007, *ApJ*, submitted (arXiv:0705.0003v1)
- Claret, A. 2004, *A&A*, 428, 1001
- Droege, T. F., Richmond, M. W., & Sallman, M. 2006, *PASP*, 118, 1666
- Fortney, J. J., Marley, M. S., & Barnes, W. 2007, *ApJ*, 659, 1661
- Fressin, F., Guillot, T., Morello, V., & Pont, F. 2007, *A&A*, in press (arXiv:0704.1919)
- Gaudi, B. S. 2005, *ApJ*, 628, L73
- Gillon, M. et al. 2007, *A&A*, in press (arXiv:0705.2219v2)
- Guillot, T., Santos, N. C., Pont, F., Iro, N., Melo, C., & Ribas, I. 2006, *A&A*, 453, L21
- Høg, E. et al. 2000, *A&A*, 355, L27
- Holman, M. J. et al. 2007, *ApJ*, in press (arXiv:0704.2907)
- Kovács, G., Zucker, S., & Mazeh, T. 2002, *A&A*, 391, 369
- Kovács, G., Bakos, G. Á., & Noyes, R. W. 2005, *MNRAS*, 356, 557
- Kovács, G., & Bakos, G. Á. 2005, astro-ph/0508081

- Latham, D. W. 1992, in IAU Coll. 135, Complementary Approaches to Double and Multiple Star Research, ASP Conf. Ser. 32, eds. H. A. McAlister & W. I. Hartkopf (San Francisco: ASP), 110
- Mandel, K., & Agol, E. 2002, ApJ, 580, L171
- Mandushev, G., et al. 2005, ApJ, 621, 1061
- Marcy, G. W., & Butler, R. P. 1992, PASP, 104, 270
- Noyes, R. W., Weiss, N. O., & Vaughan, A. H. 1984, ApJ, 287, 769
- Ochsenbein, F., Bauer, P., & Marcout, J. 2000, A&AS, 143, 23
- Pál, A., & Bakos, G. Á. 2006, PASP, 118, 1474
- Queloz, D., et al. 2001, A&A, 379, 279
- Saar, S. H., & Donahue, R. A. 1997, ApJ, 485, 319
- Santos, N. C. et al. 2002, A&A, 392, 215
- Sato, B. et al. 2005, ApJ, 633, 465
- Southworth, J., Wheatley, P. J., & Sams, G. 2007, MNRAS, in press (arXiv:0704.1570)
- Sozzetti, A., Torres, G., Charbonneau, D., Latham, D. W., Holman, M. J., Winn, J. N., Laird, J. B., & O'Donovan, F. T. 2007, ApJ, in press (arXiv:0704.2938)
- Stempels, H. C., Collier Cameron, A., Hebb, L., Smalley, B., & Frandsen, S. 2007, MNRAS, in press (arXiv:0705.1677v1)
- Torres, G., Konacki, M., Sasselov, D. D., & Jha, S. 2005, ApJ, 619, 558
- Valenti, J. A., & Fischer, D. A. 2005, ApJS, 159, 141
- Valenti, J. A., & Piskunov, N. 1996, A&AS, 118, 595
- Vogt, S. S. et al. 1994, Proc. SPIE, 2198, 362
- Yi, S. K., Demarque, P., Kim, Y.-C., Lee, Y.-W., Ree, C. H., Lejeune, T., & Barnes, S. 2001, ApJS, 136, 417

Table 1. Relative radial velocity measurements of HAT-P-3.

BJD (2,400,000+)	RV (m s <sup>-1</sup> )	$\sigma_{RV}$ (m s <sup>-1</sup> )	Phase
54187.01101 . . . . .	-38.9	1.5	0.051
54187.12931 . . . . .	-67.4	1.6	0.092
54187.97909 . . . . .	-78.9	1.8	0.385
54188.05795 . . . . .	-59.3	1.3	0.412
54188.98084 . . . . .	+75.9	1.4	0.730
54189.06253 . . . . .	+75.9	1.4	0.759
54189.11203 . . . . .	+73.9	1.5	0.776
54250.85697 . . . . .	-48.1	2.1	0.069
54278.86111 . . . . .	+65.2	2.9	0.727

Table 2. Stellar parameters for HAT-P-3.

Parameter	Value	Source
$T_{\text{eff}}$ (K) . . . . .	$5185 \pm 46$	SME <sup>a</sup>
[Fe/H] . . . . .	$+0.27 \pm 0.04$	SME
$\log g_{\star}$ (cgs) . . . . .	$4.61 \pm 0.05$	SME
$v \sin i$ (km s <sup>-1</sup> ) . . . . .	$0.5 \pm 0.5$	SME
$M_{\star}$ ( $M_{\odot}$ ) . . . . .	$0.936^{+0.036}_{-0.062}$	Y <sup>2</sup> +LC+SME <sup>b</sup>
$R_{\star}$ ( $R_{\odot}$ ) . . . . .	$0.824^{+0.043}_{-0.035}$	Y <sup>2</sup> +LC+SME
$L_{\star}$ ( $L_{\odot}$ ) . . . . .	$0.442^{+0.078}_{-0.057}$	Y <sup>2</sup> +LC+SME
$M_V$ (mag) . . . . .	$5.86 \pm 0.20$	Y <sup>2</sup> +LC+SME
Age (Gyr) . . . . .	$0.4^{+6.5}_{-0.3}$	Y <sup>2</sup> +LC+SME
Distance (pc) . . . . .	$140 \pm 13$	Y <sup>2</sup> +LC+SME

<sup>a</sup>SME = ‘Spectroscopy Made Easy’ package for analysis of high-resolution spectra Valenti & Piskunov (1996). See text.

<sup>b</sup>Y<sup>2</sup>+LC+SME = Yale-Yonsei isochrones (Yi et al. 2001), light curve parameters, and SME results.

Table 3. Spectroscopic and light curve solutions for HAT-P-3, and inferred planet parameters.

Parameter	Value
Spectroscopic parameters	
$P$ (days) <sup>a</sup> .....	$2.899703 \pm 0.000054$
$T_c$ (HJD–2,400,000) <sup>a</sup> .....	$54,218.7594 \pm 0.0029$
$K$ (m s <sup>–1</sup> ) .....	$89.1 \pm 2.0$
$\gamma$ (m s <sup>–1</sup> ) .....	$-14.8 \pm 1.5$
$e$ .....	0 (adopted)
Light curve parameters	
$a/R_\star$ .....	$10.59^{+0.66}_{-0.84}$
$R_p/R_\star$ .....	$0.1109^{+0.0025}_{-0.0022}$
$b \equiv a \cos i/R_\star$ .....	$0.51^{+0.11}_{-0.13}$
$i$ (deg) .....	$87.24 \pm 0.69$
Transit duration (days) .....	$0.0858 \pm 0.0020$
Planet parameters	
$M_p$ (M <sub>Jup</sub> ) .....	$0.599 \pm 0.026$
$R_p$ (R <sub>Jup</sub> ) .....	$0.890 \pm 0.046$
$\rho_p$ (g cm <sup>–3</sup> ) .....	$1.06 \pm 0.17$
$a$ (AU) .....	$0.03894 \pm 0.00070$
$\log g_p$ (cgs) .....	$3.310 \pm 0.066$

<sup>a</sup>Held fixed from the photometric determination (§2).

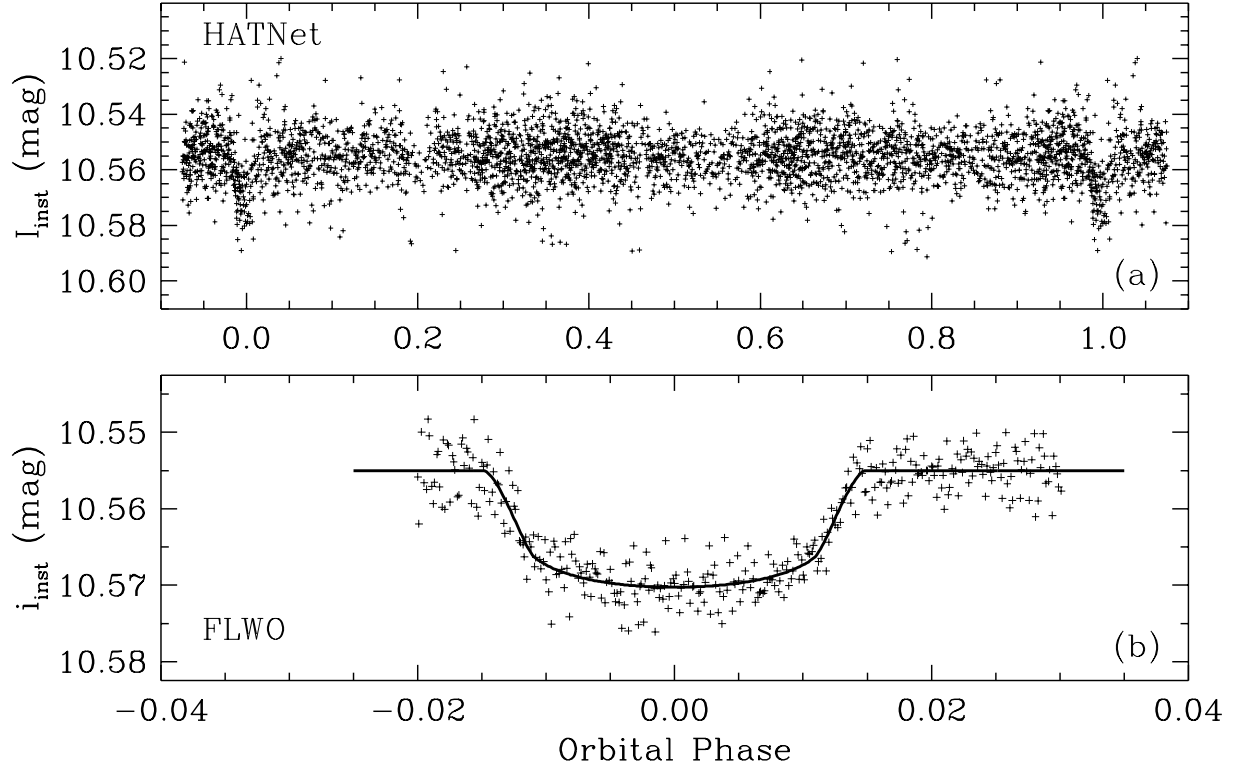


Fig. 1.— (a) Unbinned instrumental  $I$ -band discovery light curve of HAT-P-3 obtained with HATNet, folded with the period of  $P = 2.899703$  days. (b) Unbinned instrumental Sloan  $i$ -band photometry collected on UT 2007 April 27 with the 1.2-m telescope at FLWO, along with our best-fit transit model curve (see text).

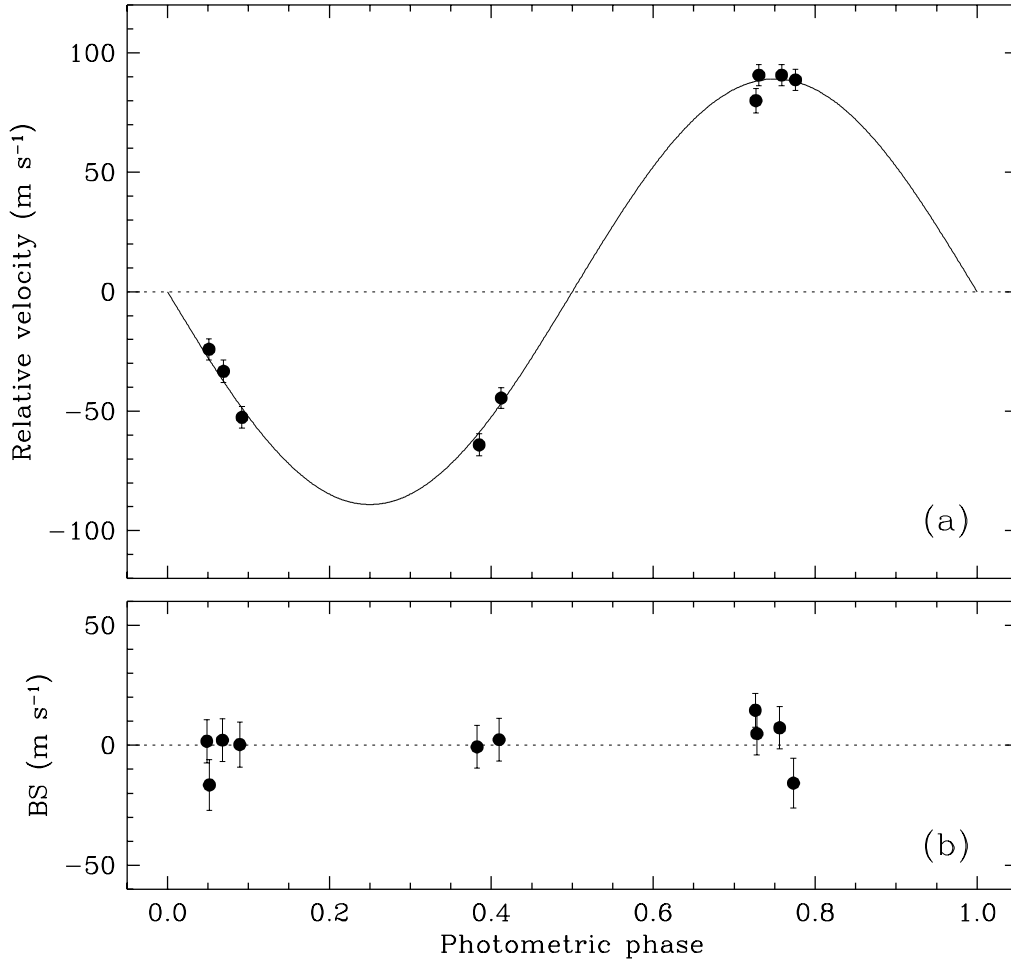


Fig. 2.— (a) Radial-velocity measurements for HAT-P-3 along with our orbital fit, shown as a function of orbital phase. The center-of-mass velocity has been subtracted. (b) Bisector spans (BS) for our 10 Keck spectra (template + 9 iodine exposures), computed as described in the text. The mean value has been subtracted, and the vertical scale is the same as in the top panel.